CrossMark

Next generation of pure titania nanoparticles for enhanced solar-light photocatalytic activity

G. Nagaraj[1] · A. Dhayal Raj[1] · A. Albert Irudayaraj[1]

Abstract

TiO_2 nanoparticles are renowned for its photocatalytic degradation. Herein, Oxygen-rich TiO_2 nanosphere and TiO_2 nanorods have been prepared by photon induced method (PIM). This facial preparation method is cost effective and produce pure anatase phased TiO_2 nanoparticles with high stability. The morphology of the prepared TiO_2 samples for various preparation times have been analyzed using HRTEM and HRSEM. As the preparation time is increased, a morphological transformation from nanorods to nanospheres is witnessed. The possible reason behind this transformation has also been discussed. The nature of the samples have been investigated using XRD, FTIR, PL, XPS and UV–Vis spectroscopy. The PIM prepared sample for 8 days show pure anatase phase stability even at a higher calcination temperature of 800 °C. This is correlated with the oxygen richness of the sample. A clear discussion regarding this enhanced phase stability is also presented here. Also, the photocatalytic activity of both the samples have been investigated through the degradation of methylene blue dye. The degradation of methylene blue under sunlight by pure TiO_2 nanosphere is quicker when compared with TiO_2 nanorods and Degussa P25. The reason for the enhanced photodegradation activity of pure TiO_2 nanospheres has also been discussed in detail.

1 Introduction

Titanium dioxide has been studied widely as a photocatalyst to deal with environmental pollution, air purification, wastewater treatment and water purification owing to its strong oxidising power, abundance, high chemical inertness, photostability and low cost [1–3]. Its structure–property relationships have been extensively investigated, and these reveal that phase type, particle size, surface, crystallinity and morphology of the photocatalyst have great impact on their photocatalytic activities [4–9]. A reasonable assumption is that both photocatalytic oxidative and reductive reactions occur simultaneously on the TiO_2 nanoparticles. Photocatalysis is the process of a photoreaction in the presence of a catalyst. The most used photocatalysts are semiconductors [10–12]. Under the irradiation of light, electrons in the semiconductor are excited from the valence band to the conduction band if the energy of light exceeds its band gap and positive holes are created in the valence band. The generation of electron–hole pairs is supported by continuous absorption of a photon. The electron–hole pairs can generate free radicals, such as hydroxyl radical, and participate in successive secondary reactions. However, its wide band gap could be activated only by the UV irradiation. To reduce the band gap and improve the photocatalytic property under visible light, considerable experimental efforts, such as doping and precursor modification (H_2O_2) have been carried out [13–20]. Recently, Etacheri et al. reported that the visible-light photocatalytic activity of undoped TiO_2 was achieved by increasing the amount of oxygen in TiO_2 [21]. However, they have modified the TiO_2 precursor using H_2O_2. This work, proposes that the band gap of TiO_2 can efficiently be reduced by novel preparation method (PIM) by introducing excess oxygen into pure TiO_2.

There are several methods to prepare anatase phased pure TiO_2 with stability up to 700 °C to remove pollution through photocatalytic degradation under UV light [22–26]. Herein, new photon induced method is adapted to prepare oxygen-rich, pure TiO_2 nanoparticles with high-temperature stability up to 800 °C to remove pollution through photocatalytic degradation under visible light. This is really a very novel result with high phase stability and visible light degradation

✉ A. Dhayal Raj
dhayalraj03@gmail.com

1 PG and Research Department of Physics, Sacred Heart College, Tirupattur, Vellore District, Tamilnadu 635601, India

when compared to those reported earlier. In this communication, a facile precipitation route for synthesizing oxygen-rich anatase phased pure TiO_2 with very low band gap (3.08 eV) has been reported. In addition, the TiO_2 nanoparticles calcinated at 800 °C exhibit excellent photocatalytic activity in the degradation of organic contaminants. The enhanced stability and low band gap results in easy absorption of visible light and thereby, easy excitation of the electrons from the valence band to the conduction band.

2 Experimental

2.1 Photon induced method

In the typical formation of the photocatalyst, titanium tetra isopropoxide was added into double distilled water, which resulted in precipitation of hydrolyzed titanium species. On exposing to photons, the electrons in the titania (TiO_2) get excited from the valence band to the conduction band to generate electron–hole pairs. The hole created in the valence band can react and break apart the water molecule to H_2 and O_2. Etacheri et al. modified the titanium precursor with H_2O_2 in order to reach oxygen-rich TiO_2. H_2O_2 is an oxidizing agent and hence it facilitates the formation of O_2–TiO_2 (oxygen rich TiO_2) [21]. Rao et al. [27], and Yang et al. [28], have reported that water splits up in the presence of a photocatalyst into hydrogen and oxygen through reduction and oxidation reactions as given below.

Oxidation : $H_2O \rightarrow 4H^+ + O_2 + 4e^-$

Reduction : $4H^+ + 4e^- \rightarrow H_2$
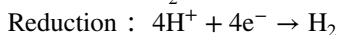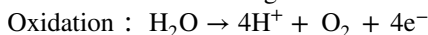
In our case, the oxygen formed by the splitting up of water acts as an oxidizer resulting in the formation of oxygen-rich TiO_2. This is confirmed through the increase in phase stability as the reaction time is increased. Which in turn suggests that prolonged exposure to photon, increases the oxygen content in the sample thus increasing the anatase phase stability of the sample.

2.2 Preparation of pure TiO₂ catalysts

The reagents used in this study were titanium tetra-isopropoxide purchased from sigma and double distilled water. In the typical experiment 2 ml of titanium tetra-isopropoxide ($Ti(OPr)_4$) was added into 600 ml of Double Distilled water. The solution was then stirred for 7 h under 250 W Halogen light and placed in an open atmosphere for 6 days (solar irradiation) then 3 ml ammonia solution was added drop by drop until the pH reached 12. The powder thus obtained was dried and calcinated at 800 °C for 1 h. A similar procedure was adopted for the other sample except that the reaction time was changed from 6 to 8 days. In order to compare the
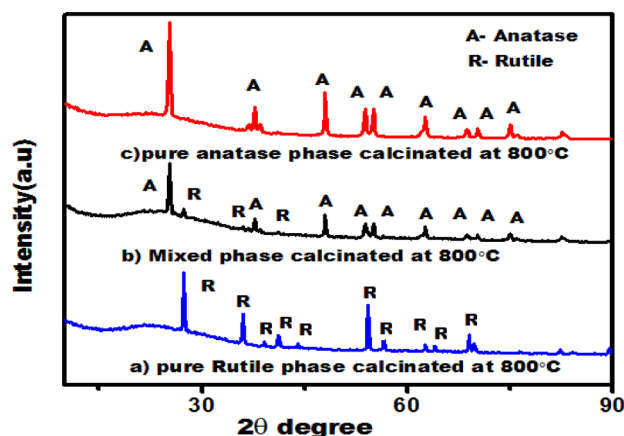

Fig. 1 XRD patterns of 800 °C calcinated *a* Standard Degussa P25 pure TiO_2, *b* 6 days prepared pure TiO_2 and *c* 8 days prepared pure TiO_2

results with the control sample, Degussa P25 sample was purchased and calcinated at 800 °C.

2.3 Characterization

Powder X-ray diffraction (XRD) pattern of catalysts was recorded on a Bruker D8 Advance powder X-ray diffractometer with Cu-Kα ($\lambda = 1.5406$ Å). Particle size and morphology were ascertained via (FEI Quanta FEG 200) high resolution scanning electron microscope. High-resolution transmission electron microscopic (HRTEM) images were recorded with transmission electron microscope JEOL 300 kV. X-ray photoelectron spectroscopy (XPS) measurements were carried out using a multi-probe system (Omicron Nanotechnology, Germany) equipped with a dual Mg/Al X-ray source and a hemispherical analyzer operating in constant analyzer energy mode. The spectra were obtained with a 50 eV pass energy for both survey scan and individual scans. The Mg Kα X-ray source was operated at 300 W and 15 kV. The base pressure in the analyzing chamber was maintained at 1×10^{-10} bar. with FTIR analysis was carried out using Perkin Elmer Spectrum Version 10.4.00 and the UV-visible spectrum was recorded via Varian Cary Bio 50 spectrometer.

3 Results and discussion

3.1 X-ray diffraction analysis

XRD analysis was carried out inorder to examine the crystalline structure, phase and crystallite size of P25 sample and PIM prepared samples. Appearance of multiple peaks suggest that all three samples have polycrystalline nature.

The XRD pattern in Fig. 1a, corresponds to Degussa P25 sample. The well resolved peaks are in match with those in JCPDS # 21-1276 revealing the existence of rutile phase in the P25 sample. Figure 1b, shows the XRD pattern of pure TiO_2 prepared by PIM for 6 days. The peaks indicate that the obtained samples were TiO_2 nanoparticles consisting of anatase and rutile phases. Figure 1b clearly shows the coexistence of two titania polymorphs, containing peaks corresponding to rutile phase matching with JCPDS #21-1276 and anatase phase matching with JCPDS # 21-1272. The existence of rutile phase in the 6 days prepared sample was readily discernible from its (110) diffraction peak located at 2θ of 27.7° in the XRD pattern and the presence of anatase phase can be also easily identified from its (101) peak located at 2θ of 25.6°, because no overlapping of these peaks with any other peaks from anatase or rutile occurred. It is clearly evident that the sample prepared for 6 days contains both anatase and rutile phases. The peaks in Fig. 1b have been indexed accordingly as A (Anatase) and R (Rutile) [29]. However, the XRD pattern in Fig. 1c, corresponding to the PIM prepared sample for 8 days clearly shows the existence of pure anatase phased TiO_2 with peaks having 2θ at 25.6°, 37.7°, 48.4°, 53.4°, 62.8°, 68.3°, 70.3° and 75.4° corresponding to (101), (004), (200), (105), (211), (204), (116), (220) and (215) planes respectively [30]. From Fig. 1c, it may be noted that only anatase phased TiO_2 has been found in this sample. This may be due to the increased oxygen content in the sample which has increased the anatase phase stability [21]. The average crystallite size are calculated using the Scherer equation $D = k\lambda/\beta\cos\theta$, where β is the full width on half maximum of the diffraction peak, k = 0.89 is the shape factor, θ is the Braggs angle of the peak, and λ is the X-ray wavelength corresponding to the Cu Kα radiation. The average crystallite size of Degussa P25 sample was found to be 130 nm, PIM sample prepared for 6 days was found to be 35 nm and PIM sample prepared for 8 days was found to be 26 nm.

3.2 FTIR analysis

The FTIR spectra of the TiO_2 samples for Degussa P25 sample is shown Fig. 2a and the FTIR spectra of the oxygen-rich TiO_2 prepared by PIM for 6 and 8 days are shown in Fig. 2b, c) respectively. In Fig. 2b, the peaks corresponding to Ti–O–O and C–O bonds were identified at 685 and 1021 cm^{-1} and in Fig. 2c, the peaks corresponding to Ti–O–O and C–O bonds were identified at 670 and 1013 cm^{-1} respectively, for the oxygen-rich pure TiO_2 samples [21, 31]. No such peaks was observed for the Degussa P25 and only Ti–O bonds were observed at 722 cm^{-1} as shown in Fig. 2a [32]. The peak around 1627 cm^{-1} correspond to the hydroxyl groups of molecular water and the broad peak at 3407 cm^{-1} is correlated to stretching vibration
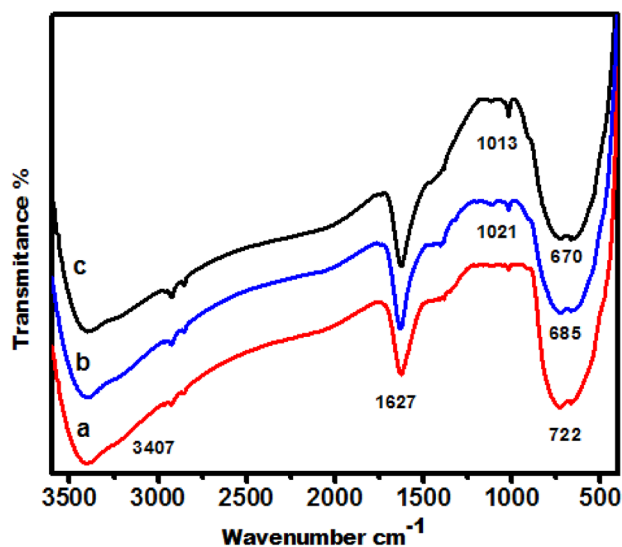

Fig. 2 FTIR spectrum of TiO_2 calcinated at 100 °C for *a* Standard Degussa P25, *b* 6 days prepared pure TiO_2 and *c* 8 days prepared pure TiO_2
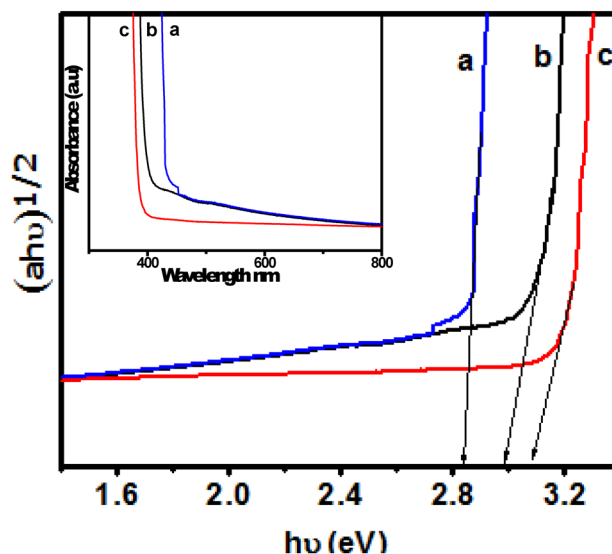

Fig. 3 Transformed KM function vs. hυ plot of 800 °C calcinated *a* Standard Degussa P25 (rutile phase), *b* 6 days prepared pure TiO_2 (mixed phase) and *c* 8 days prepared pure TiO_2 (anatase phase)

of C–OH group are shown in Fig. 2a–c [31–33]. The small peaks at 2810 and 2890 cm^{-1} in the spectrum may be attributed the CH_2 stretching vibration [34].

3.3 UV–Vis absorbance and Photoluminescence analysis

Room temperature optical absorbance spectra of Degussa P25 sample, 6 days prepared nanorods sample and 8 days
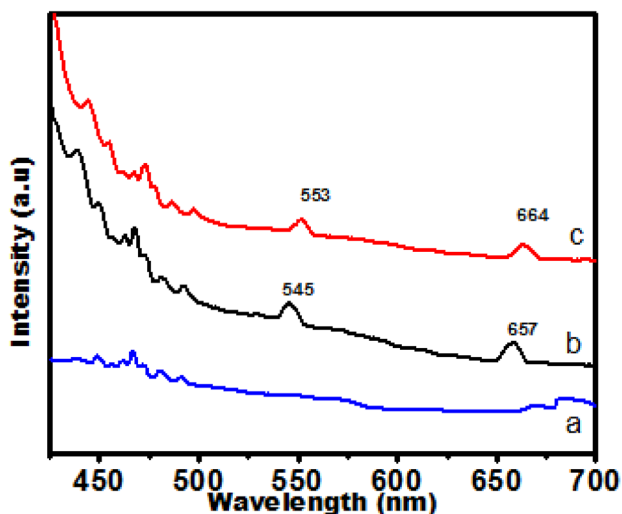
Fig. 4 The photoluminescence spectrum of 800 °C calcinated *a* Standard Degussa P25, *b* 6 days prepared pure TiO$_2$ and *c* 8 days prepared pure TiO$_2$

prepared nanosphere samples thermally decomposed at 800 °C for 1 h are shown as inset in Fig. 3. The band gap of the samples is calculated using the formula,

$$\alpha h\upsilon = A \left(h\upsilon - E_g\right)^{1/2}$$

where hυ is the photon energy, α is the optical absorption coefficient, E_g is the indirect band gap, and A is a constant. The band gap of the pure TiO$_2$ sample was measured by plotting $(\alpha h\upsilon)^{1/2}$ as a function of photon energy, and the extrapolating the linear portion of the curve as shown in Fig. 3a–c. The band gap calculated for calcinated Degussa P25, 6 and 8 days grown samples were found to be 2.83, 2.99

and 3.08 eV respectively. These band gap values are smaller then the band gap 3.2 eV reported for standard Degussa P25 sample with anatase phase. Hence it can be concluded that, oxygen-rich TiO$_2$ prepared by this novel method has narrow band gap when compared to standard Degussa P25 sample. Photoluminescence spectra were recorded at room temperature on the pure TiO$_2$ samples prepared by PIM. The photoluminescence spectra of the sample prepared for 6 days show peaks at 545 and 657 nm corresponding to green and red emissions whereas 8days prepared sample show peaks shifted to 553 and 664 nm corresponding to green and red emission respectively, as shown in Fig. 4b, c, while for Degussa P25 sample, no such peaks are found as can be seen from Fig. 4a.

3.4 HRSEM and HRTEM morphology analysis

High-resolution scanning electron microscopic, image corresponding to the calcinated TiO$_2$ samples prepared for 6 days show nanorods like structures and 8 days show nanosphere like structures as shown in Fig. 5b, c, while the image of Degussa P25 sample calcinated at 800 °C in Fig. 5a shows more agglomeration. From the images of Degussa P25 it is evident that the particles in the images are not clear. Hence high-resolution transmission electron microscopic is required for further investigations. Figure 6(a,b and c) correspond to the high-resolution transmission electron microscopy images of the calcinated Degussa P25, 6 days prepared and 8 days prepared TiO$_2$ samples. It is evident that Degussa P25 shows more agglomerated, 6 days prepared sample shows rods like morphology with a width 50 nm and length 130 nm, while those prepared for 8 days show sphere like morphology with particles size ranging between 30 and 40 nm. Link et al. have obtained nanoparticles from nanorods through photothermal heating. In our case,
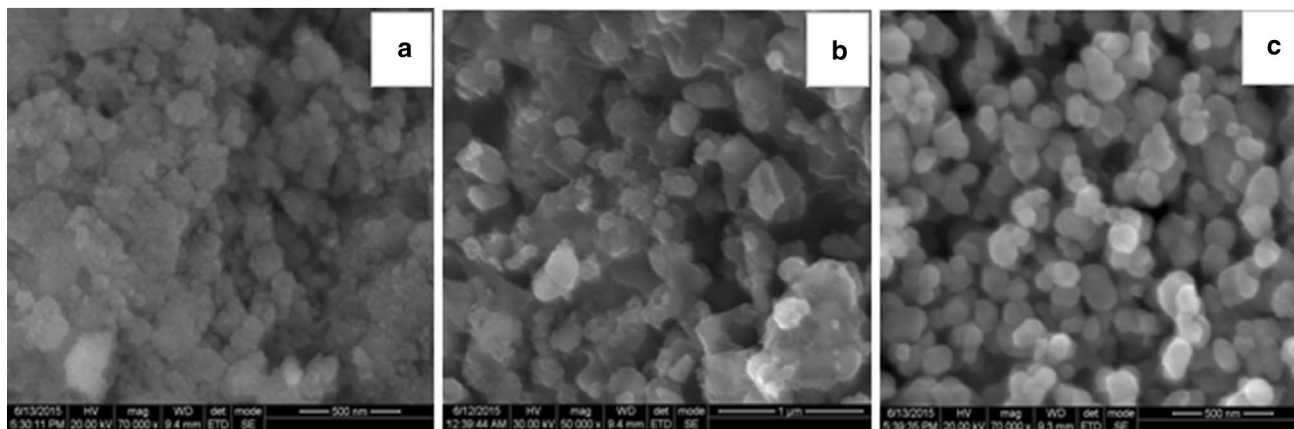

Fig. 5 HR-SEM micrographs of TiO$_2$ calcinated at 800 °C. **a** Standard Degussa P25, **b** 6 days prepared pure TiO$_2$ and **c** 8 days prepared pure TiO$_2$
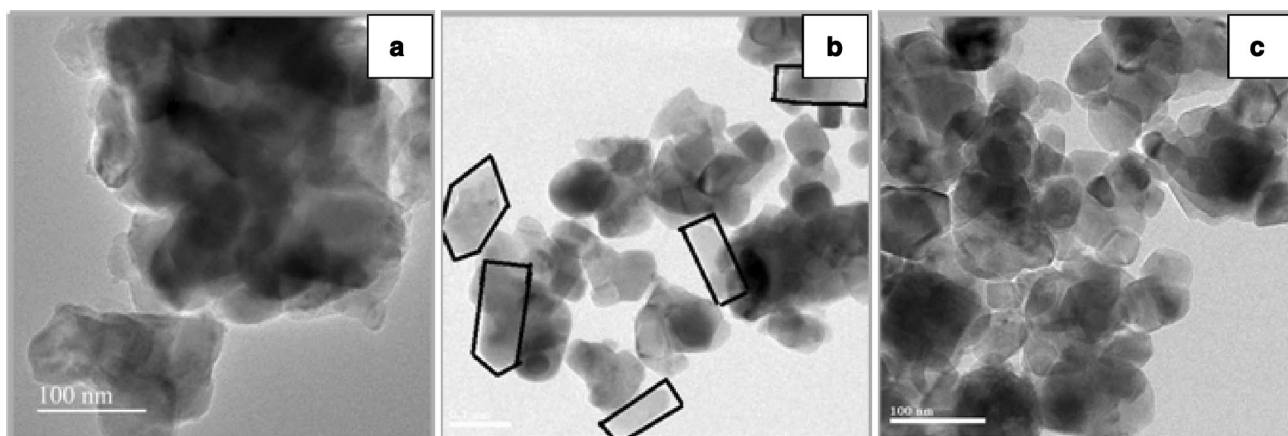
Fig. 6 HR-TEM micrographs of 800 °C calcinated TiO$_2$. **a** Standard Degussa P25, **b** 6 days prepared pure TiO$_2$ and **c** 8 days prepared pure TiO$_2$
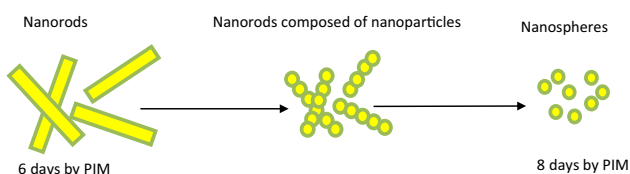

Fig. 7 Schematic and formation illustration of nanspheres from nanorods

the prolonged exposure to photons may have resulted in increased heating. This may be the reason for breaking up of rods into particles. The transformation of nanorods to nanospheres due to heat has also been discussed in earlier reports [35–40]. The possible schematic behind the transformation of nanords to nanosphere has been presented in Fig. 7.

3.5 XPS analysis

Figure 8 shows the XPS spectrum corresponding to the Ti2p and O1s spectra. The chemical states of Ti and O species in the TiO$_2$ sample prepared by PIM for 8 days has been investigated using X-ray photoelectron spectroscopy. The existence of Ti in its Ti^{4+} chemical state may be confirmed through the appearance of Ti2p$_{3/2}$ and Ti2p$_{1/2}$ peaks at 462.23 and 467.93 eV, respectively [41–43]. Moreover, the 5.7 eV splitting between these two bands confirms that Ti exists mainly in the Ti^{4+} state in the 8 days prepared TiO$_2$ sample [43, 44]. Quantification of the result revealed a O$_2$:Ti ratio of 2.398. Tan et al. and Chai et al. have reported that the O$_2$:Ti ratio for the control sample is 2.315 [42, 43]. Thus comparing our result with those reported Tan and Chai et al.
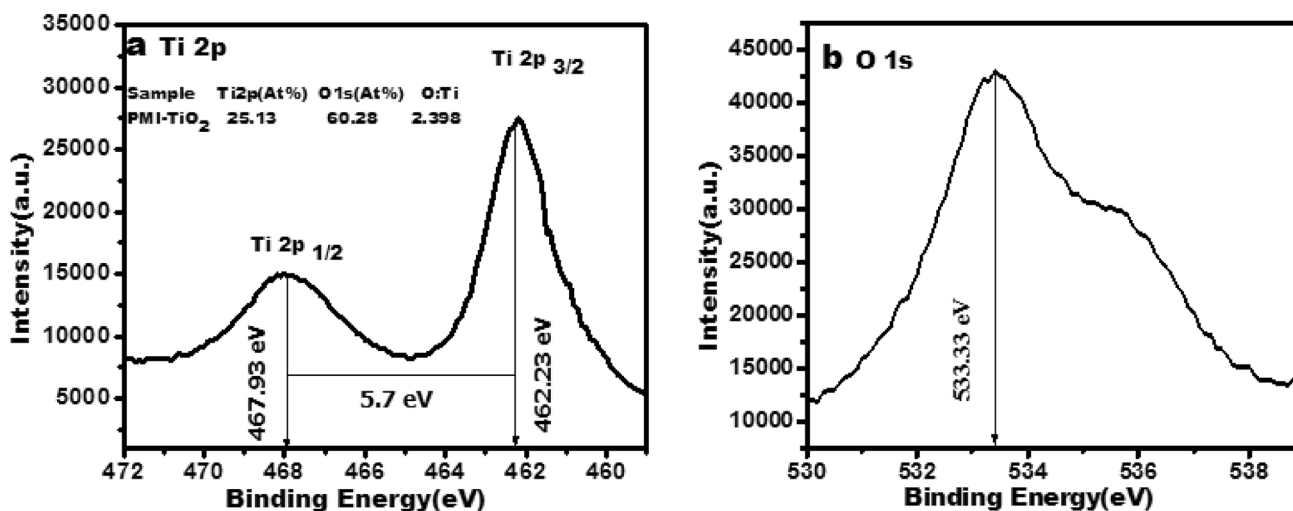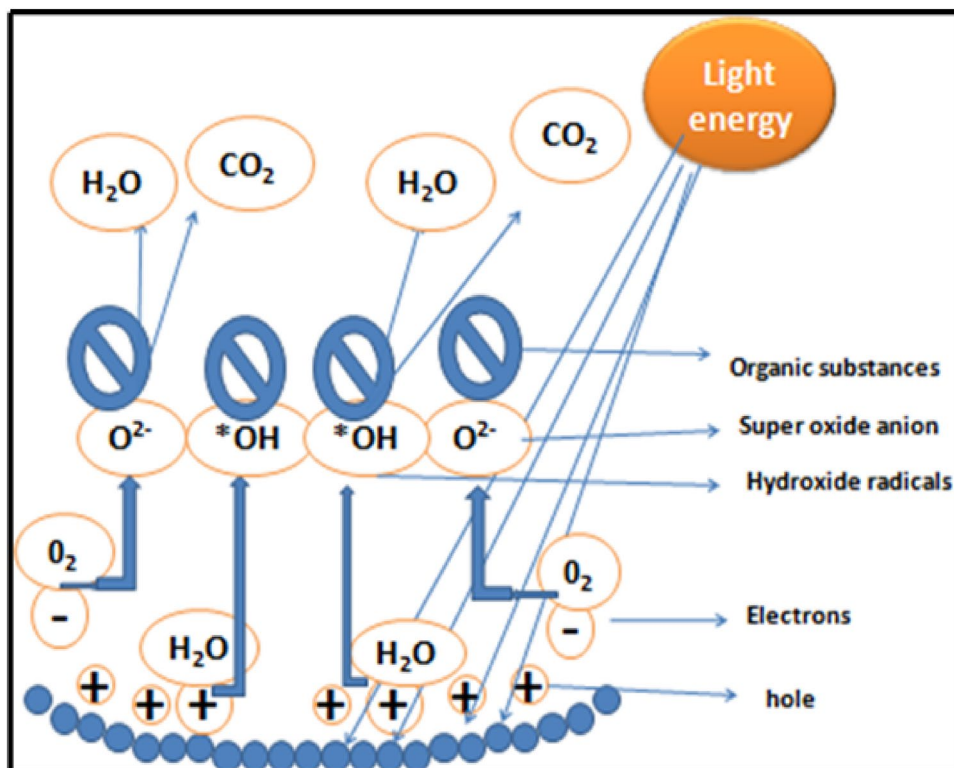

Fig. 8 XPS spectra of calcinated at 800 °C **a** Ti 2p and **b** O 1s

Fig. 9 Photocatalytic dye degradation mechanism

it is evident that the sample obtained by PIM after 8 days is oxygen-rich TiO_2.

3.6 Photocatalytic activity

The energy of the photons available in solar radiation was absorbed by TiO_2 nanoparticles. After acquiring enough energy, the valence electrons in the TiO_2 nanoparticles move to the excited state leaving back holes in the valence band. These holes react with water to produce hydroxyl radicals while the excited electrons reduce the dioxygen molecule to from superoxide radicals. These radicals are capable of breaking up of chemical bonds in various dyes. Thus TiO_2 nanoparticles have become one of the best photocatalyst to address environmental pollution. Figure 9 shows the photocatalytic mechanism involved in anatase TiO_2. The photodegradation of methylene blue (1 mmol/l) was carried out in a 500 ml beaker in the presence of TiO_2 photocatalyst (0.05 g/l) under the irradiation of sunlight. The photocatalytic degradation curves corresponding to Degussa P25, nanorods and nanospheres samples are shown in Fig. 10a–c respectively. Figure 11a–c shows the time vs. ln A_0/A graph. It can be clearly seen that Degussa P25 TiO_2 powder when exposed to sunlight degrade methylene blue (MB) within 40 min, 6 days prepared TiO_2 nanorods when exposed to sunlight degrade MB within 40 min and 8 days prepared TiO_2 nanospheres when exposed to sunlight degrade MB within 40 min. Therefore, it can be seen that pure TiO_2 nanospheres show better degradation compared than TiO_2 nanorods and Degussa P25. The reduction in photodegradation time when exposed to sunlight may be accounted to the increased surface to volume ratio of the nanospheres when compared to nanorods and also the pure anatase phase of the nanospheres. The absorption peak of MB dye corresponds to the wavelength 665.2 nm. The reduction in the intensity of the absorption peak inturn means the reduction in the concentration of MB dye [45–48].

3.7 Enhanced photocatalytic activity of pure anatase phase titania

There are several factors that have contributed to the enhanced photocatalytic activity of oxygen-rich TiO_2 nanoparticles prepared by PIM. The main factor which increases the photocatalytic activity is the narrowing of band gap in the oxygen rich sample (Fig. 12). Classical band gap structures corresponding to the titania with oxygen vacancy (Degussa P25) and Oxygen-rich titania (PIM prepared samples) are presented in Fig. 12. The reported band gap values for TiO_2 control sample (Degussa P25) is 3.2 eV while for the sample prepared for 8 days by PIM showed 3.08 eV. This narrowing of band gap when compared to Degussa P25, also enhances the visible light
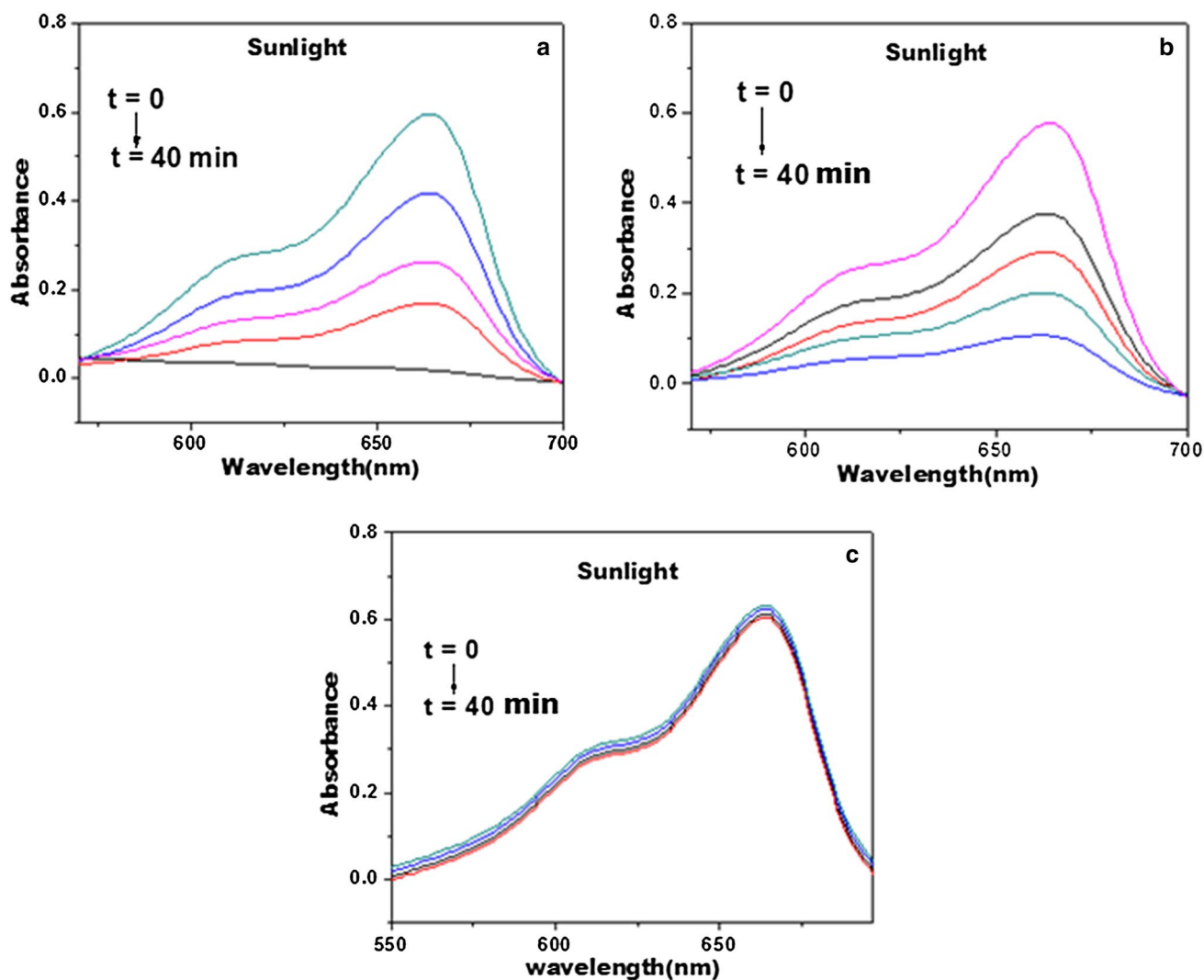
Fig. 10 Photocatalytic degradation of methylene blue dye in the presence of 800 °C calcinated TiO$_2$. **a** 8 days prepared pure TiO$_2$, **b** 6 days prepared pure TiO$_2$ and **c** Standard Degussa P25

absorption. The excess of oxygen present in the oxygen rich sample serve as electron scavengers that could reduce the recombination rate of electron–hole pairs [21]. Thus, the excess oxygen in the PIM prepared titania prolongs the life time of electrons and holes thereby facilitating them to participate in the process of preparing superoxide and hydroxyl radicals. Also PIM prepared samples show smaller particle size when compared to Degussa P25. The smaller particle size is related to enhanced surface to volume ratio which inturn enhances the photocatalytic activity of the PIM samples. To the best of our knowledge, there is no prior reports on enhanced photocatalytic activity under visible light by a dopant-free TiO$_2$ without undergoing precursor modification. Thus, the oxygen-rich TiO$_2$ prepared by photon induced method will be a

promising material for photocatalytic application compared to standard Degussa P25 sample reported earlier.

4 Conclusions

Pure TiO$_2$ nanospheres and nanorods were successfully grown by the facial photon induced method. The structural and stability of the pure TiO$_2$ nanospheres and nanorods prepared with different reaction time have been systematically investigated. The sample prepared with 6 days and calcinated at 800 °C shows nanorod like morphology and possesses a mixed phase corresponding to anatase and rutile, a band gap of 2.99 eV and the sample prepared with 8 days and calcinated at 800 °C show nanosphere like morphology with pure anatase phase and a
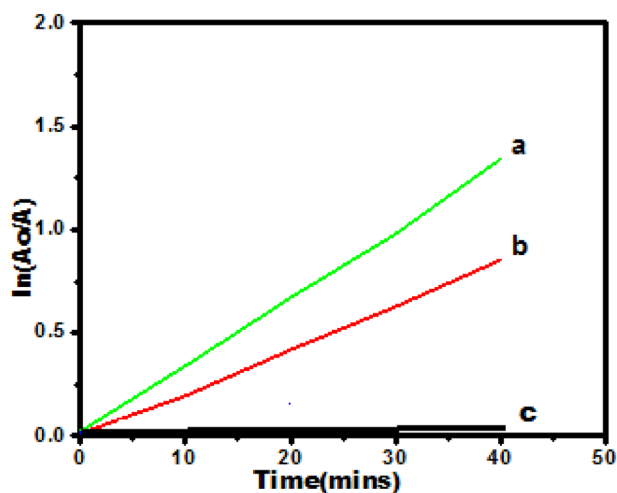
Fig. 11 Linear transforms $-\ln(A_o/A)$ versus irradiation time for methylene blue degradation under solar light of 800 °C calcinated TiO_2 *a* 8 days prepared pure TiO_2 *b* 6 days prepared pure TiO_2 and *c* Standard Degussa P25
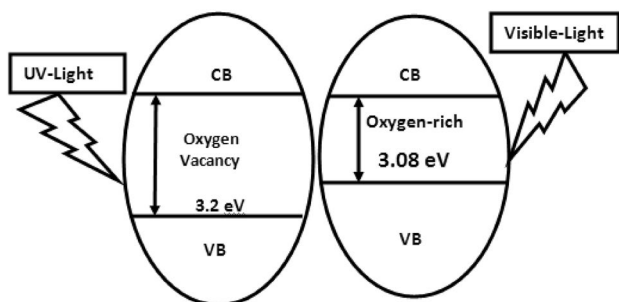

Fig. 12 Oxygen vacancy and oxygen-rich band gap

band gap 3.08 eV, While Degussa P25 sample calcinated at 800 °C show more agglomerate morphology with pure rutile phase and a band gap 2.83 eV. This clearly shows that reaction time plays a vital role in tuning the phase and band gap. From the photocatalytic analysis, it is concluded that Degussa P25 TiO_2 sample having a pure rutile phase with a crystalline size of 130 nm shows very no visible light photocatalytic activity, 6 days prepared the nanorods sample having a mixed phase with a crystalline size of 35 nm shows visible light photocatalytic activity, while 8 days prepared the nanosphere sample exhibiting pure anatase phase with a crystalline size 26 nm shows an enhanced visible light photocatalytic activity. However, both the samples enhanced stability and visible light activity than Degussa P25.

Compliance with ethical standards

References

1. A. Fujishima, T.N. Rao, D.A. Tryk, Titanium dioxide photocatalysis. J. Photochem. Photobiol. C **1**, 1–21 (2000)
2. A. Fujishima, K. Hashimoto, T. Watanabe, *TiO2 Photocatalysis: Fundamentals and Applications*, 1st edn. (BKC, Tokyo, 1999)
3. K. Honda, A. Fujishima, Electrochemical photolysis of water at a semiconductor electrode. Nature **238**, 37–38 (1972)
4. N. Sakai, R. Wang, A. Fujishima, T. Watanabe, Effect of ultrasonic treatment on highly hydrophilic TiO_2 surfaces. Langmuir **14**, 5918–5920 (1998)
5. Z. Lin, A. Orlov, R.M. Lambert, M.C. Payne, New insights into the origin of visible light photocatalytic activity of nitrogen-doped and oxygen-deficient anatase TiO_2. J. Phys. Chem. B **109**, 20948–20952 (2005)
6. R.R. Besca, J. Kiwi, Effect of rutile phase on the photocatalytic properties of nanocrystalline titania during the degradation of p-coumaric acid. Appl. Catal. B **16**, 19–29 (1998)
7. L. Kavan, M. Grtzel, S.E. Gilbert, Electrochemical and photoelectrochemical investigation of single-crystal anatase. J. Am. Chem. Soc. **118**, 6716–6718 (1996)
8. E. Beyers, P. Cool, E.F. Vansant, Anatase formation during the synthesis of mesoporous titania and its photocatalytic effect. J. Phys. Chem. B **109**, 10081–10083 (2005)
9. S.S. Hosseinpour-Mashkani, A. Sobhani-Nasab Investigation the effect of temperature and polymeric capping agents on the size and photocatalytic properties of $NdVO_4$ nanoparticles. J. Mater. Sci.: Mater. Electron. **28**(21), 16459–16466 (2017)
10. X. Huang, L. Meng, M. Du, Y. Li, TiO_2 nanorods: hydrothermal fabrication and photocatalytic activities. J. Mater. Sci.: Mater. Electron. **27**, 1–5 (2016). https://doi.org/10.1007/s10854-016-4687-y
11. Z. Liu, Y. Zheng, T. Gao, J. Zhang, X. Sun, G. Zhou, Fabrication of anatase TiO_2 tapered tetragonal nanorods with designed {100}, {001} and {101} facets for enhanced photocatalytic H_2 evolution. Int. J. Hydrog. Energy. **42**(34), 21775–21785 (2017)
12. Z. Yan Liu, M. Li, M.J. Green, Y.Y. Li, X. Chen, Titanium dioxide nanomaterials for photocatalysis. J. Phys. D **50**(19), 193003 (2017)
13. X. Chen, S.S. Mao, Titanium dioxide nanomaterials:synthesis, properties, modification, and application. Chem. Rev. **107**, 2891–2959 (2007)
14. X.Z. Liu, P.F. Fang, Y. Liu, Effect of holmium doping on the structure and photocatalytic behaviour of TiO_2-based nanosheets. J. Mater. Sci. **49**, 8063–8073 (2014)
15. A. Asahi, T. Morikawa, T. Ohwaki, Visible-light photocatalysis in nitrogen-doped titanium oxide. Science **293**, 269–271 (2001)
16. J.Y. Shen, Y.N. Wu, L. Fu, preparation of doped TiO_2 nanofiber membranes through electrospinning and their application for photocatalytic degradation of malachite green. J. Mater. Sci. **49**, 2303–2314 (2014)
17. H. Pan, X. Qiu, I.N. Ivanov, Fabrication and characterization of brookite-rich, visible light-active TiO_2 films for water splitting. Appl. Catal. B **93**, 90–95 (2009)
18. Z.S. Lin, A. Oriov, R.M. Lambert, New insights into the origin of visible light photocatalytic activity of nitrogen-doped and oxygen-deficient anatase TiO_2. J. Phys. Chem. B **109**, 20948–20952 (2005)

19. H. Pan, B. Gu, Z. Zhang, Phase dependent photocatalytic ability of TiO_2: a first principles study. J. Chem. Theory Comput. **5**, 3074–3078 (2009)

20. H. Tong, S.X. Ouyang, Y.B. Bi, Nano photocatalytic materials: possibilities and challenges. Adv. Mater. **24**, 229–251 (2012)

21. V. Etacheri, M.K. Seery, S.J. Hinder, S.C. Pillai, Oxygen rich titania: a dopant free, high temperature stable, and visible light active anatase photocatalyst. Adv. Funct. Mater. **21**, 3744–3752 (2011)

22. C. Miner, F. Catozzo, E. Pelizzetti, Role of adsorption in photocatalyzed reactions of organic molecules in aqueous titania suspensions. Langmuir **8**, 481–486 (1992)

23. S. Salmin, A. Shamali, Photocatalytic degradation of methylene blue in the presence of TiO_2 catalyst assisted solar radiation. Aust. J. Basic Appl. Sci. **7**, 172–176 (2013)

24. V. Augugliaro, L. Palmisano, A. Sclafani, C. Minero, E. Pelizzetti, Photocatalytic degradation of phenol in aqueous titanium dioxide dispersions. Toxicol. Environ. Chem. **16**, 89–95 (1988)

25. S.M. Hosseinpour-Mashkani, A. Sobhani-Nasab, Green synthesis and characterization of $NaEuTi_2O_6$ Nanoparticles and its photocatalyst application. J. Mater. Sci.: Mater. Electron. **28**, 4345 (2017)

26. M. Salavati-Niasari, F. Soofivand, A. Sobhani-Nasab, M. Shakouri-Arani, M. Hamadanian, S. Bagheri (2017) Facile synthesis and characterization of $CdTiO_3$ nanoparticles by Pechini sol-gel method. J. Mater. Sci.: Mater. Electron. 28(20), 14965–14973 (2017)

27. S.R. Urmimala Maitra, C.N.R. Lingampalli, Rao, Artificial photosynthesis and the splitting of water to generatehydrogen. Curr. Sci. **106**, 518–526 (2014)

28. H. Lingling Yang, T. Zhou, D. Fan, Zhang, Semiconductor photocatalysts for water oxidation: current status and challenges. Phys. Chem. Chem. Phys. (2014). https://doi.org/10.1039/C4CP00246F

29. W.-K. Wang, J.-J. Chen, X. Zhang, Y.-X. Huang, W.-W. Li, H.-Q. Yu, Self-induced synthesis of phase-junction TiO_2 with a tailored rutile to anatase ratio below phase transition temperature. Sci. Rep. **6**, (2016). https://doi.org/10.1038/srep20491

30. M.A. Khan, M.S. Akhtar, O.-B. Yang, Synthesis, characterization and application of sol-gel derived mesoporous TiO_2 nanoparticles for dye-sensitized solar cells. Sol. Energy **84**, 2195–2201 (2010)

31. Y. Gao, Y. Masuda, Z. Peng, T. Yonezawa, K. Koumoto, Room temperature deposition of a TiO_2 thin film from aqueous peroxotitanate solution. J. Mater. Chem. **13**, 608–613 (2003)

32. S. Nayak, B. Sahoo, T.K. Chakia, D. Khastgir, Facile preparation of uniform barium titanate ($BaTiO_3$) multipods with high permittivity: impedance and temperature dependent dielectric behavior. RSC Adv. **4**,1212–1224 (2014)

33. W.-S. Wang, D.-H. Wang, W.-G. Qu, L.-Q. Lu, A.-W. Xu, Large ultrathin anatase TiO_2 nanosheets with exposed 001 facets on graphene for enhanced visible light photocatalytic activity. J. Phys. Chem. C **116**(37), 19893–19901 (2012)

34. M.S. Sher Shah, A.R. Park, K. Zhang, J.H. Park, P.J. Yoo, Green synthesis of biphasic TiO_2-reduced graphene oxide nanocomposites with highly enhanced photocatalytic activity. ACS Appl. Mater. Interfaces **4**(8), 3893–3901 (2012)

35. S. Link, Z.L. Wang, M.A. El-Sayed, How does a gold nanorod melt. J. Phys. Chem. B **104**, 7867–7870 (2000)

36. A. Dhayal Raj, P. Suresh Kumar, D. Mangalaraj, N. Ponpandian, A. Albert Irudayaraj, Q. Yang, Gas sensing behaviour of high surface Co_3O_4 micro/nano structures synthesized by simple sonication process. Sens. Lett. **10**, 825–831 (2012)

37. S. Karim, M.E. Toimil-Molares, A.G. Balogh, W. Ensinger, T.W. Cornelius, E.U. Khan, R. Neumann, Morphological evolution of Au nanowires controlled by Rayleigh instability. Nanotechnology **17**, 5954–5959 (2006)

38. J.L. Jiménez-Pérez, R. Gutiérrez Fuentes, R. Sánchez-Sosa, M.G. Zapata Torres, Z.N. Correa-Pacheco, J.S. Ramírez, Thermal diffusivity study of nanoparticles and nanorods of titanium dioxide (TiO_2) and titanium dioxide coated with cadmium sulfide (TiO_2CdS). Mater. Sci. Semicond. Process. **37**, 62–67 (2015)

39. S.H. Nam, D.W. Ju, J.H. Boo (2014) Comparison of photovoltaic properties of TiO_2 electrodes prepared with nanoparticles and nanorods. J. Nanosci. Nanotechnol. 14(12), 9406–10

40. T. Balkan, A.S. Sarac, Morphological effect of composite TiO_2 nanorod-TiO_2 nanoparticle/PEDOT:PSS electrodes on triiodide reduction. Express Polym. Lett. **11**(2), 106–116 (2017)

41. H. Cao, B. Li, J. Zhang, F. Lian, X. Kong, M. Qu, Synthesis and superior anode performance of TiO_2 reduced graphene oxide nanocomposites for lithium ion batteries. Mater. Chem. **22**, 9759 (2012)

42. L.-L. Tan, W.-J. Ong, S.-P. Chai, A.R. Mohamed, Band gap engineered, oxygen-rich TiO_2 for visible light induced photocatalytic reduction of CO_2. Chem. Commun. **50**, 6923 (2014)

43. L.-L. Tan, W.-J. Ong, S.-P. Chai, B.T. Goh, A.R. Mohamed, Visible-light-active oxygen-rich TiO_2 decorated 2D graphene oxide with enhanced photocatalytic activity toward carbon dioxide reduction. Appl. Catal. B **179**, 160–170 (2015)

44. M.S. Arif Sher Shah, K. Zhang, A.R. Park, K.S. Kim, N.-G. Park, J.H. Park, P.J. Yoo, Single-step solvothermal synthesis of mesoporous Ag–TiO_2–reduced graphene oxide ternary composites with enhanced photocatalytic activity. Nanoscale **5**, 5093–5101 (2013)

45. R.S. Dariani, A. Esmaeili, A. Mortezaali, S. Dehghanpour, Photocatalytic reaction and degradation of methylene blue on TiO_2 nano-sized particles. Optik **127**, 7143–7154 (2016)

46. M.A. Ahmed, E. Emad, Z.H. El-Katori, Gharni, Photocatalytic degradation of methylene blue dye using Fe_2O_3/TiO_2 nanoparticles prepared by sol–gel method. J. Alloy. Compd. **553**, 19–29 (2013)

47. C.-H. Wu, J.-M. Chern, Kinetics of photocatalytic decomposition of methylene blue. Ind. Eng. Chem. Res. **45**, 6450–6457 (2006)

48. W. Chuanxi Yang, G. Dong, Y. Cui, X. Zhao, X. Shi, B. Xia, W. Tang, Wang, Highly efficient photocatalytic degradation of methylene blue by P_2ABSA–modified TiO_2 nanocomposite due to the photosensitization synergetic effect of TiO_2 and P2ABSA. RSC Adv. **7**, 23699 (2017)